JBC Papers in Press. Published on October 10, 2018 as Manuscript RA118.004891
The latest version is at http://www.jbc.org/cgi/doi/10.1074/jbc.RA118.004891

Insulin and 20-hydroxyecdysone oppose each other in the regulation of phosphoinositide-dependent kinase-1 expression during insect pupation

Jing Pan[1], Yu-Qin Di[1], Yong-Bo Li, Cai-Hua Chen, Jin-Xing Wang, Xiao-Fan Zhao[*]

Shandong Provincial Key Laboratory of Animal Cells and Developmental Biology, School of Life Sciences, Shandong University, Jinan, Shandong 250100, China

Running title: Insulin and 20E cross talk to regulate insect pupation

1 Equal contribution authors.
∗ Corresponding author: Xiao-Fan Zhao, E-mail: xfzhao@sdu.edu.cn. GenBank accession number of PDK1: MG563224.

Keywords: insulin, 20-hydroxyecdysone, PDK, FoxO, pupation, autophagy, apoptosis, cell proliferation, bollworm, insect development

Abstract

Insulin promotes larval growth of insects by stimulating the synthesis of the steroid hormone 20-hydroxyecdysone (20E), which induces pupation and apoptosis. However, the mechanism underlying the coordinate regulation of insect pupation and apoptosis by these two functionally opposing hormones is still unclear. Here, using the lepidopteran insect and serious agricultural pest *Helicoverpa armigera* (cotton bollworm) as a model, we report that phosphoinositide-dependent kinase-1 (PDK1) and forkhead box O (FoxO) play key roles in these processes. We found that the transcript levels of the *PDK1* gene are increased during the larval feeding stages. Moreover, *PDK1* expression was increased by insulin, but repressed by 20E. dsRNA-mediated *PDK1* knockdown in the *H. armigera* larvae delayed pupation and resulted in small pupae and also decreased *AKT/protein kinase B* expression and increased *FoxO* expression. Furthermore, the *PDK1* knockdown blocked midgut remodeling and decreased 20E levels in the larvae. Of note, injecting larvae with 20E overcame the effect of the *PDK1* knockdown and restored midgut remodeling. *FoxO* overexpression in an *H. armigera* epidermal cell line (HaEpi) did not induce apoptosis, but promoted autophagy and repressed cell proliferation. These results reveal crosstalk between insulin and 20E and that both hormones oppose each other's activities in the regulation of insect pupation and apoptosis by controlling *PDK1* expression and, in turn, *FoxO* expression. We conclude that sufficiently high 20E levels are a key factor for inducing apoptosis during insect pupation.

Introduction

The insulin/insulin-like growth factor (IGF) signaling (IIS) pathway is a conserved pathway in animals (1). Mammalian insulin is produced in the islets of Langerhans in the pancreas, and insect IGFs are produced in the brain and various tissues. Although the production organs for mammalian insulin and insect IGFs are different, the structures of insulin and IGFs are similar and consist of two peptide chains, namely the A and B chains (2). Bombyxin is the first insulin-like peptide (ILP) identified in *Bombyx mori* (3). In insects, up to 38 ILPs have been identified in each species (4). The function of the IIS pathway is to promote growth (5,6). In mammals, the IIS pathway regulates the metabolism of carbohydrates, fats, and proteins by promoting the absorption of glucose from the blood into the liver and fat and skeletal muscle cells (7). In *Drosophila*, the IIS pathway promotes cell growth and proliferation (5) (8). The effect of the IIS on metabolism of insects is little known.

Phosphoinositide-dependent kinase-1 (PDK1) is a central mediator in various

pathways, including the insulin pathway, by phosphorylating many AGC kinases, such as protein kinase B (AKT/PKB), p70 ribosomal S6 kinase (S6K), p90 ribosomal S6 kinase (RSK), protein kinase N (PKN), and all protein kinase C (PKCs) (9). In the insulin pathway, PDK1 phosphorylates AKT/PKB (10), which then phosphorylates the transcription factor forkhead box O (FoxO). The phosphorylated FoxO is located in the cytoplasm and loses its transcription activity in the nucleus (11,12). Thus, insulin can promote cell proliferation and repress apoptosis (13). Repression of the IIS pathway influences the morphology of *Drosophila* (14). Repression of insulin/TOR signaling in *Drosophila* suppresses larval growth and delays pupation time (15). Overexpression of PDK1 in *Drosophila* increases cell and organ size (9,14). However, there is limited information on the involvement and mechanism of PDK1 during pupation in lepidopteran insects.

In insects, pupation is promoted by 20-hydroxyecdysone (20E), which is a steroid hormone that promotes insect molting and metamorphosis (16). 20E combines with its nuclear receptor EcRB1 to form the EcRB1/USP1 heterodimeric transcription complex (17,18), which regulates the expression of genes in the 20E pathway, including hormone receptor 3 (*HR3*) (19) and broad (*Br*) (20) that initiate metamorphosis and midgut remodeling. Midgut remodeling is controlled by 20E, and it includes imaginal midgut formation after the proliferation of regenerative cells and larval midgut programmed cell death (PCD). During larval midgut PCD, the color of the larval midgut changes to red, and it is finally degraded through PCD (21-23). In *B. mori*, autophagy and apoptosis successively occur during larval midgut PCD (24).

Insulin and 20E cross talk to regulate insect development. Insulin promotes 20E production by promoting insect growth to critical body weight, and the prothoracic glands (PGs) grow larger to produce more 20E for metamorphosis (25,26). In *D. melanogaster*, overexpression of FoxO in the PGs delays ecdysone biosynthesis and critical weight (27). Human insulin can induce AKT phosphorylation in *Helicoverpa armigera*, thereby inducing FoxO phosphorylation and cytoplasm localization. In contrast, 20E represses AKT phosphorylation, thereby repressing FoxO phosphorylation and inducing FoxO nuclear localization (28). Because PDK is a key protein kinase in the insulin pathway, we hypothesized PDK is involved in the crosstalk between insulin and 20E.

Using *H. armigera*, the cotton bollworm, as a model, we identified PDK1 as a key factor for the coordinated regulation of insect midgut remodeling and pupation by insulin and 20E. Our results showed that PDK1 plays key roles in insect pupation by participating in the insulin pathway. Insulin and 20E cross talk by counteractively regulating *PDK1* mRNA levels to regulate insect pupation.

Results

Insulin promoted PDK1 expression and 20E repressed PDK1 expression- To examine the involvement of *PDK1* in insect development, the expression profile of *PDK1* was examined (Fig.1). The qRT-PCR results showed that *PDK1* was expressed in the epidermis, fat body, and midgut. The transcript levels of *PDK1* increased during the feeding stages of the sixth instar at 6 h to sixth instar at 24 h (6th-6h to 6th-24h) in the fat body, epidermis, and midgut and then decreased from the sixth instar at 48 h and were low during the metamorphic stages (6th-72h to 6th-120h) (Fig. 1A), indicating PDK1 transcript levels are correlated with feeding.

HaEpi, a cell line established in our laboratory from the 5th instar larval epidermis (29), was used to examine the regulation of *PDK1* mRNA levels by insulin and 20E. After insulin stimulation for 3 h, *PDK1* transcripts were upregulated in a dose-dependent manner from 2 μg/ml to 5 μg/ml (Fig. 1B). By stimulation with 2 μg/ml of insulin, *PDK1* transcripts were upregulated from 1 h to 3 h gradually, and it then recovered to the base levels (Fig. 1C). These results suggested that insulin increases the mRNA levels of *PDK1* in a dose-dependent manner in a short period.

Because the 20E titer is higher at metamorphic molting in lepidopteran insects (16), HaEpi cells were treated with exogenous 20E to examine the effects of regulation of 20E on *PDK1* expression. We found that 5 μM 20E decreased *PDK1* transcript levels significantly in 6 h (Fig. 1D),

and 5 μM 20E consistently decreased *PDK1* transcript levels significantly from 3 h to 24 h (Fig. 1E). The in vivo results of the larval midgut also confirmed that insulin promoted *PDK1* expression and 20E repressed *PDK1* expression (Figs. 1F, G, H, and I). These results suggested that 20E consistently decreases the expression of *PDK1* in a dose-dependent manner.

PDK1 determined pupation time and pupa weight- To study the functions of *PDK1* during *H. armigera* growth and pupation, *PDK1* was knocked down by injecting dsRNA against *PDK1* into sixth-instar 6-h larvae. The larvae formed small pupae (Fig. 2A). Statistical analysis showed no differences in the pupation rate after injection with *dsPDK1* or *dsGFP*, with 75% survival and 25% death (Fig. 2B); however, the *dsPDK1* injection prolonged pupal duration and delayed the initiation time of pupation for 34 h on average (recorded from sixth instar 0 h) (Fig. 2C). Moreover, the pupal weight decreased to an average of 0.16 g when compared with 0.32 g of the *dsGFP* injection control (Fig. 2D). These results suggested that PDK1 is critical for pupation.

To understand how *PDK1* knockdown delayed pupation, the downstream genes in the insulin pathway were detected. The qRT-PCR assay showed that the expression of *AKT* decreased and that of *FoxO* increased after knockdown of *PDK1* in the midgut (Fig. 2E). Therefore, PDK1 affects the transcript levels of *AKT* and *FoxO* as with the cell line.

Knockdown of PDK1 in the larvae repressed midgut remodeling and decreased 20E titer- To examine the effects of *PDK1* knockdown on midgut remodeling, we dissected the larvae 90 h after dsRNA injection of 6th-instar 6 h larvae (6th-6-h larvae). All midguts of the *dsGFP*-injected larvae appeared red color (23), which implies the midgut was entering PCD (30); in contrast, all midguts of the *dsPDK1*-injected larvae appeared yellow, indicating the midgut did not enter PCD (Fig. 3A). Hematoxylin–eosin (HE) staining showed that the larval midgut separated from the imaginal midgut after *dsGFP* injection, indicating the occurrence of midgut remodeling. In contrast, the imaginal midgut did not form after *dsPDK1* injection (Fig. 3B), confirming that *PDK1* knockdown repressed midgut remodeling.

The detailed structure of the midgut was observed using transmission electron microscopy (TEM) after *PDK1* knockdown. The number of typical autophagosomes, which are two-membraned and contain degenerating cytoplasmic organelles or cytosol (31), increased in the midgut after *PDK1* knockdown in the midgut when compared with the *dsGFP* control (Figs. 3C and D), suggesting *PDK1* knockdown arrested the midgut at the autophagic stage.

Because 20E is the key factor for promotion of midgut remodeling, the 20E titer was suspected to be insufficient on the basis of decreased body weight after *PDK1* knockdown. Therefore, we determined the 20E titer in the whole larvae 90 h after injection with dsRNA and found that the 20E titer had decreased significantly after injection with *dsPDK1* (Fig. 3E). These results suggested that knockdown of *PDK1* decreases the 20E titer, thereby repressing midgut remodeling.

Complementation of 20E rescued the effect of PDK1 knockdown- To prove that knockdown of *PDK1* repressed apoptosis because of the low titer of 20E, 20E (500 ng/larva) was injected into sixth-instar 6-h larvae after injection with *dsPDK1* for 48 h. When compared with the DMSO control, the larval midgut appeared red (23,32) (Fig. 4A) and the larval midgut separated from the imaginal midgut (Fig. 4B), which indicated that complementation of 20E recovered midgut remodeling when *PDK1* was knocked down.

PDK1 was knocked down in HaEpi to confirm it caused autophagy, as observed in the midgut. The autophagy-related protein, microtubule-associated protein 1 light chain 3 (LC3, one isoforme of ATG8) (33) was overexpressed as a fusion protein with the cell-penetrating TAT peptide and red fluorescence protein RFP (His-TAT-RFP-LC3-His) to detect autophagosomes in HaEpi (34). The TAT peptide helped the fusion protein His-TAT-RFP-LC3-His to enter the cells (35), RFP showed red fluorescence, and LC3 protein indicated the puncta of autophagosomes by its location in the autophagosome membrane (31). His-TAT-RFP-LC3-His indicated that LC3 formed puncta after *PDK1* was knocked

down in *dsPDK1* + DMSO-treated cells, but 5 μM 20E blocked the formation of the LC3 puncta significantly in *dsPDK1* + 20E-treated cells (Figs. 4C and D).

In contrast, caspase-3 activity was detected in few *dsPDK1* + DMSO-treated cells, but caspase-3 activity was detected in 85% *dsPDK1* + 20E-treated cells (Figs. 4E and F). The efficiency of interference of *PDK1* in HaEpi was significant (Fig. 4G). These results suggested that *PDK1* interference indeed induces autophagy, but could not induce apoptosis, and 20E is the key factor for inducing apoptosis.

Overexpression of FoxO-induced autophagy, but not apoptosis **-** We observed that *PDK* knockdown caused an increase in *FoxO* mRNA levels in the larval midgut; however, the midgut was arrested at the autophagic stage, which implied that FoxO could induce autophagy, but not apoptosis without sufficient 20E. To confirm that FoxO induced autophagy, we detected the transformation of LC3-I to LC3-II (phosphatidyl ethanolamine form) by using western blot, which indicates autophagy (36). FoxO-GFP was confirmed to be overexpressed in the HaEpi cells (Fig. 5A). Overexpression of FoxO-GFP-His increased the LC3-II level, whereas addition of 5 μM 20E for 72 h decreased the LC3-II level significantly (Fig. 5B and C).

RFP-LC3 was overexpressed in HaEpi to indicate the autophagosomes to further confirm that overexpression of FoxO induces autophagy. RFP-LC3 is a fluorescent protein that can reveal autophagosomes (34,37,38). The number of autophagosomes increased after overexpression of FoxO-GFP-His; however, addition of 20E for 72 h decreased the autophagosomes (Figs. 5D and E). The negative control by the RFP tag had fewer autophagosomes (Fig. 5F). These results confirmed that FoxO promotes autophagy, but treatment with 5 μM 20E for 72 h caused disappear of autophagosomes.

FoxO-His was overexpressed in HaEpi (Fig. 6A) to evaluate the role of FoxO in apoptosis. Caspase-3 activity was detected in 18% cells in His-tag overexpression cells after addition of 20E, with DMSO treatment as a solvent control, suggesting 20E-induced apoptosis. Similarly, caspase-3 activity was detected in 18% cells in FoxO-His overexpressed cells after addition of 20E (Figs. 6B and C). Flow cytometry analysis further confirmed that His-tag overexpression and FoxO-His overexpression induced 3-4% cell apoptosis, but 20E supplementation induced 18% cell apoptosis (Figs. 6D and E). These results confirmed that overexpression of *FoxO* alone cannot induce apoptosis.

Overexpression of FoxO repressed cell proliferation- *PDK* knockdown in the larvae produced small pupae and repressed the formation of imaginal midgut cells, which was accompanied by an increase in *FoxO* mRNA levels. Thus, FoxO was hypothesized to be involved in the repression of cell proliferation. To verify the assumption, cell proliferation was detected by 5-ethynyl-2′-deoxyuridine (EdU) staining after overexpression of FoxO-GFP by using the pIEx-FoxO-GFP-His plasmid in HaEpi. The results showed that the proliferative signal EdU was detected in the nucleus of GFP-overexpressing cells when compared with the 20E-treated cells (5 μM for 72 h), suggesting the GFP-overexpressing cells proliferate normally and 20E represses cell proliferation. However, a very low EdU signal was detected in the FoxO-GFP-overexpressing cells, regardless of DMSO treatment or 5 μM 20E treatment (Figs. 7A and B); this suggested that FoxO overexpression results in an effect similar to that after 20E treatment to repress cell proliferation.

PDK1 **knockdown inhibits insulin-induced Akt and FoxO phosphorylation**

To verify the function of PDK1 in the insulin pathway in *H. armigera*, we analyzed the involvement of PDK1 in insulin-induced Akt and FoxO phosphorylation in HaEpi by overexpression of Akt fused with RFP-His and FoxO fused with GFP-His in the cells, respectively. Western blot showed insulin-induced phosphorylation of both Akt and FoxO. However, knockdown of *PDK1* blocked insulin-induced Akt and FoxO phosphorylation significantly (Figs. 8A, a and B, b). These results confirmed that insulin, via PDK1, induced Akt and FoxO phosphorylation in *H. armigera*. Moreover, insulin induced FoxO translocation to the cytosol from the nucleus by GFP co-fluorescence indication. However, knockdown of *PDK1* blocked

insulin-induced FoxO translocation to the cytosol (Fig. 8C). These results confirmed that PDK1 is involved in the insulin pathway in *H. armigera*.

Discussion

IGF intensifies the cell proliferation and inhibition of cell apoptosis via the PI3K/Akt signaling pathway (39), whereas the steroid hormone 20E promotes apoptosis during insect metamorphosis (40). It is intriguing how these functionally counteractive hormones regulate insect pupation and apoptosis coordinately. Our study showed that PDK1 plays a critical role in the crosstalk between insulin and the steroid hormone 20E. PDK1 is necessary for 20E synthesis. PDK1 functions as a repressor of *FoxO*. 20E represses *PDK1* expression to release *FoxO* expression for autophagy, and 20E finally promotes apoptosis.

PDK1 is necessary for 20E synthesis to regulate insect metamorphosis and apoptosis- Repression of insulin and reduced ecdysone levels have similar effects on larval pupation (41). Insulin promotes insect body growth and PG growth, thereby promoting 20E synthesis (25). The 20E titer is lower than 0.5 μg/ml during the feeding stage, but it increases to about 5 μg/ml in the hemolymph during the metamorphic stage of *Antheraea mylitta* (42). In this study, we found that repression of the insulin pathway via knockdown of *PDK1* in the larvae resulted in a decrease in the 20E titer from 1.5 μg/g to 0.1 μg/g, suggesting that insulin via PDK1 regulates the increase in 20E levels.

Larval midgut PCD has been proven to be apoptosis-mediated during metamorphosis in the lepidopteran insects *Bombyx mori* (43) and *H. armigera* (30). Autophagy was observed before apoptosis in the midgut of *B. mori* (44,45). In *H. armigera*, a high concentration of 20E promotes apoptosis, but a low concentration of 20E induces autophagy; autophagy is switched to apoptosis when a high concentration of 20E triggers Ca^{2+} influx (34). We found the decreased 20E titer after *PDK1* knockdown could not trigger midgut remodeling and pupation. By complementation of 20E in the larvae, midgut remodeling was recovered, confirming that 20E is the critical factor that promotes midgut remodeling. Our study confirmed that the insulin and 20E interplay for regulating metamorphosis is a common mechanism in insects.

PDK1 plays a significant role in repressing FoxO mRNA levels- FoxO is a transcription factor that regulates diverse processes, such as energy homeostasis, apoptosis, and cellular differentiation, and life span. FoxO is phosphorylated by AKT and arrested in the cytoplasm to lose its transcriptional function under insulin regulation (13). The phosphorylation of AKT and FoxO in *H. armigera* is induced by insulin and repressed by 20E in HaEpi, and the non-phosphorylated FoxO is localized in the nucleus (28). However, little is known about the transcriptional regulation of FoxO, compared to its post-translational modifications (46). Previous studies have reported that 20E represses FoxO phosphorylation and promotes FoxO nuclear translocation in *Drosophila* (41) and *Bombyx* (47). In *H. armigera*, 20E via its nuclear receptor EcRB1 promotes FoxO expression (28). In this study, we found that *PDK1* knockdown caused an increase in FoxO mRNA, which suggests PDK1 is a repressor of FoxO. PDK1 plays a key role in the insulin pathway by regulating AKT phosphorylation (10); thus, *FoxO* transcription is possibly repressed by the insulin pathway.

FoxO regulates the life span of *Drosophila* (48,49). We found that *PDK1* knockdown increased FoxO mRNA levels, elongated the larval stage, and delayed pupation time, suggesting that FoxO plays a role in the elongated larval life span. Further analyses of the HaEpi cells showed that the overexpressed FoxO induced autophagy. This phenomenon is correlated to the finding that FoxO promotes autophagy-related gene expression in animals (50). However, overexpressed FoxO did not induce apoptosis. In addition, we found that, although *PDK1* knockdown decreased *AKT* expression and increased *FoxO* expression, midgut PCD was not induced when 20E was insufficient. Therefore, apoptosis is controlled by 20E in a FoxO-independent manner, which is inconsistent with the finding that FoxO induces apoptosis in humans (51,52). This may be because 20E is necessary for inducing high cellular Ca^{2+} levels for apoptosis (53) and the

transformation of autophagy to apoptosis in insects (34).

20E via repressing *PDK1* mRNA levels to antagonize the insulin pathway- Insulin and 20E had an antagonistic effect on the regulation of glycogen mobilization and showed a similar effect on carbohydrate reserves in *B. mori (54)*. A lower 20E concentration could not repress insulin function (30), and a higher 20E concentration is critical for antagonizing insulin function in *H. armigera* (55). The ecdysone counteracts the growth-promoting action of insulin by mediating nuclear localization of dFOXO in *Drosophila* (41). 20E promotes FoxO expression and represses FoxO phosphorylation by upregulating PTEN (phosphatase and tensin homolog) expression, which represses Akt and FoxO phosphorylation in *H. armigera* (28). Here, we showed that 20E counteracts the insulin pathway by repressing *PDK1* expression in a dose-dependent manner. 20E repressed the insulin pathway via a negative feedback mechanism when it was increased to a critical titer by insulin. This is consistent with the finding that increased 20E levels negatively repress insulin function (56). However, the mechanism that 20E represses PDK1 expression needs further study in future work.

Conclusions

PDK1 was highly expressed during the larval feeding stage to promote cell proliferation and larval growth under insulin regulation. 20E titer was increased alone with larval growth; therefore repressed *PDK1* expression in a dose-dependent manner. PDK1 repressed *FoxO* expression. FoxO induces autophagy but not apoptosis under insufficient 20E titer conditions. A sufficient 20E titer is the key factor for triggering metamorphosis and midgut apoptosis (Fig. 8D).

MATERIAL AND METHODS

Experimental animal- *Helicoverpa armigera* specimens were raised on an artificial diet, according to a previous study (57), in our laboratory. The larvae were maintained at 27 °C with 60–70% relative humidity and conditions of 14-h light and 10-h dark.

HaEpi culture-

HaEpi was established in our laboratory from the 5th instar larval epidermis (29). The cell line has been used to study the hormonal pathways of 20E, JH, and insulin by RNAi or overexpression (28). The cells were cultured in cell culture flasks with a monolayer at the bottom and maintained at 27 °C. In every tissue culture flask, 4 ml of Grace's medium supplement with 10% heat-inactivated fetal bovine serum (FBS) was added, and subculture was performed once a week.

Bioinformatic analysis of PDK1- The cDNA of *PDK1* was identified after transcriptome sequencing of HaEpi cells in our laboratory. The reading frame of *PDK1* was analyzed using ExPASy Translate (http://web.expasy.org/translate/). The molecular weight (MW) and isoelectric point (pI) were predicted using ExPASy Compute pI/Mw (http://web.expasy.org/compute_pi/). The protein domain was predicted using SMART (http://smart.embl-heidelberg.de/).

RNA interference (RNAi) in the larvae and HaEpi cell line- Double-stranded RNA (dsRNA) was prepared using *PDK1* cDNA as the template (1719 bp) with the MEGAscript^{TM} RNAi kit (Ambion, Austin, Texas, USA) and primers (PDK1RNAiF and PDK1RNAiR sequences in Table 1). A single long *dsRNA* was used for *H. armigera* and produced good results in our previous study (58,59) and other lepidopteran insects (60). Thus, a long dsRNA was used (870 bp from 352 to 1222 bp) for the experiments. The long dsRNA was cleaved into multiple siRNAs in the cells by intracellular RNase to target multiple sites of the gene (61) (62). We checked the RNAi ratio by using the primers PDK1-RTF and PDK1-RTR (Table 1). For the RNAi experiment using the larvae, dsRNA was diluted to 400 ng/μl with phosphate-buffered saline (PBS; 140 mM NaCl, 2.7 mM KCl, 10 mM Na_2HPO_4, 1.8 mM KH_2PO_4), and 5 μl was injected into the hemocoel of the sixth-instar 6-h larvae. The control larvae were injected with 2 μg of *dsGFP*. In every experiment, 30 larvae were injected with dsRNA, and the injection was repeated twice over a 24-h interval. HaEpi was cultured at 27 °C in Grace's medium supplemented with 10% FBS to almost 80% density. Then, the cells were incubated in 2 μg dsRNA and 10 μl lipofectamine in 1 ml of Grace's medium supplemented with 10% FBS after 6 h.

Hormone treatment for the larvae and HaEpi cell line- The stock solution for 20E (10 mg/ml, about 20 mM in dimethyl sulfoxide, DMSO) was diluted 100-fold with PBS (10 mM Na_2HPO_4, 1.8 mM KH_2PO_4, 140 mM NaCl, and 2.7 mM KCl, pH 7.4) and injected into sixth-instar 6-h larvae (100-500 ng per larva). The stock solution for human insulin (10 mg/ml) was diluted 10-fold with PBS and injected into sixth-instar 6-h (6th-6 h) larvae (0.5–5 μg per larva). HaEpi was cultured to approximately 80% density, and 20E or stock solution of human insulin (10 mg/ml in PBS) was added at various concentrations or intervals. The control larvae or HaEpi cells were treated with the same amount of DMSO as the solvent control.

Detection of 20E levels- The larvae were frozen in liquid nitrogen for 5 min and homogenized sufficiently in 1 ml of 80% methyl alcohol and centrifuged at 12000 × *g* and 4 °C for 15 min. The supernatant was air-dried. Then, the 20-hydroxyecdysone Enzyme Immunoassay kit (Bertin Pharma, France) was used to measure the 20E titer, according to the manufacturer's instructions.

Real-time quantitative RT-PCR (qRT-PCR)- Total RNA was acquired from the larvae using TransZol reagent (Transgen, China). Total RNA was transcribed into first-strand cDNA as the midgut template for qRT-PCR. Then, 10 μl of the reaction mixture, containing 5 μl of SsoFast EvaGreen Supermix (Bio-Rad), 2 μl of 1 μmol/l forward primer, 2 μl of 1 μmol/l reverse primer, and 1 μl of cDNA (1:6 dilution), was used. β-actin was used for quality control (59). The data were analyzed using the following formula: $R = 2^{-(\Delta Ct\ sample\ -\ \Delta Ct\ control)}$ where R is the relative transcriptional level, ΔCt sample is the difference between the Ct of the gene and average β-actin in the experimental sample, and ΔCt control is the difference between the Ct of the gene and average β-actin in the control sample (63).

Hematoxylin-eosin staining (HE) staining and TEM- The waxing and dewaxing of the samples and HE staining were performed as described previously (30). The section was washed with running water for 1 min and stained with Scott's liquid for 1 min. Then, the section was washed with hydrochloric acid ethanol differentiation medium (70% ethanol in 1% hydrochloric acid) for 20 s, stained with Scott's liquid for 1 min, incubated with 0.5% water-soluble eosin dye solution for 30 s, and then washed with running water. Finally, the sections were sealed with 80% glycerin and observed using an Olympus BX51 fluorescence microscope (Tokyo, Japan). TEM was performed by the Servicebio Company (Wuhan, China) after the larvae were treated in the various experiments.

Overexpression of proteins in the HaEpi cells- FoxO-GFP-His, FoxO-His, or His tag proteins constructed in our laboratory (28) were overexpressed with 4 μg of pIEx-4 plasmid (Novagen) and 10 μl of QuickShuttle-enhanced transfection reagent (Biodragon Immunotechnologies Co., Ltd, Beijing, China) for 48 h in 1 ml of Grace's medium, according to the manufacturer's instructions and our previous study (34).

Western blot

The cell homogenates were separated using 12.5% sodium dodecyl sulfate-polyacrylamide gel electrophoresis (SDS-PAGE). Equal amounts of each sample (50 μg) was subjected to SDS-PAGE. The proteins were transferred to the nitrocellulose membrane (0.45 μm) by electrotransfer. The membrane was blocked with the blocking buffer (2% non-fat milk in PBS) for 1 h at room temperature. The membrane was then incubated with the primary antibody (diluted 1:5000 in the blocking buffer) against GFP or His tags (Zhong Shan Jin Qiao, Beijing, China) overnight at 4 °C and with the secondary antibody for alkaline phosphatase (Zhong Shan Jin Qiao, Beijing, China) conjugated with horse anti-mouse IgG diluted to 1:10,000 in the blocking buffer. The protein signal was visualized using 45 μl of nitroblue tetrazolium (75 mg/ml) and 35 μl of 5-bromo- 4-chloro-3-indolylphosphate (50 mg/ml; Sigma) in 10 ml of TBS in the dark at room temperature. The protein bands on the membrane were analyzed using Quantity One software (BIO-RAD, Hercules, California USA).

Detection of autophagy

The anti-rabbit polyclonal antibody against *H. armigera* LC3 was prepared to detect LC3 by performing western blot analysis, as described previously (64). The RFP-LC3-His fusion protein was overexpressed for 48 h in HaEpi by the

pIEx-4-RFP-LC3-His reporter plasmid to detect autophagosomes. A cell-penetrating TAT peptide (TATGGCAGGAAGAAGCGGAGACAGC GACGAAGA) (35) was fused with RFP and LC3 (His-TAT-RFP-LC3-His) and expressed in *E. coli* by the pET30a-TAT-RFP-LC3 plasmid to detect autophagosomes in HaEpi (34).

Detection of apoptosis

An aspartic acid proteinase called caspase-3 is a highly conserved protein that can form active caspase-3 during apoptosis (65). Thus, caspase-3 activity can be used to indicate apoptosis. The NucView™ caspase-3 assay kit (NO. 30029 Biotium, Hayward, USA) was used to detect caspase-3 activity in the HaEpi cells, according to the manufacturer's instructions. Annexin-V and propidium iodide (PI) were used to detect apoptosis by using the Annexin V-FITC Apoptosis Detection kit (GK3603, Genview, USA) and flow cytometry (Amnis). Annexin V-FITC stained the earlier apoptotic cells by binding to the membrane phosphatidylserine, and PI indicated the later apoptotic cells and dead cells by entering the cells.

Detection of cell proliferation- The 5-ethynyl-2′-deoxyuridine (EdU) kit (Ribobio, Guangzhou, China) was used to detect cell proliferation levels, according to the manufacturer's protocol. FoxO-GFP and GFP tags were overexpressed by the pIEx-4-FoxO-GFP-His and pIEx-4-GFP-His plasmids, respectively, in the HaEpi cells for 24 h. Then, the cells were treated with 5 μM of 20E for 72 h. The same volume of DMSO was used as the control.

Statistical analysis-Student's *t*-test was used for statistical analysis of the paired data. The bars represent mean ± standard deviation (SD) values of three independent biological experiments. Statistical significance was determined using two-tailed paired Student's *t*-test. Differences were considered statistically significant at $*p < 0.05$ and $**p < 0.01$. GraphPad Prism 5 (version 5.01) was used to produce the figures.

Acknowledgments

This study was supported by grants from the National Natural Science Foundation of China (31730083 and 31572328).

Conflict of interest

The authors declare that they have no conflicts of interest with the contents of this article.

Author contributions

Jing Pan did the experiments in Figures 1 to 4. Yu-Qin Di did the experiments in Figures 1 and 8. Yong-Bo Li did the experiments in Figures 5 to 7. Cai-Hua Chen helped with some of the experiments. Jing-Xing Wang and Xiao-Fan Zhao conceived and supervised this study.

References

1. Umezaki, Y., Hayley, S. E., Chu, M. L., Seo, H. W., Shah, P., and Hamada, F. N. (2018) Feeding-state-dependent modulation of temperature preference requires insulin signaling in *Drosophila* warm-sensing neurons. *Curr. Biol.* **28**, 779-787 e773
2. Mizoguchi, A., and Okamoto, N. (2013) Insulin-like and IGF-like peptides in the silkmoth *Bombyx mori*: discovery, structure, secretion, and function. *Front. Physiol.* **4**, 217
3. Nagasawa, H., Kataoka, H., Isogai, A., Tamura, S., Suzuki, A., Ishizaki, H., Mizoguchi, A., and Fujiwara, Y. (1984) Amino-terminal amino Acid sequence of the silkworm prothoracicotropic hormone: homology with insulin. *Science* **226**, 1344-1345
4. Nassel, D. R., and Vanden Broeck, J. (2016) Insulin/IGF signaling in *Drosophila* and other insects: factors that regulate production, release and post-release action of the insulin-like peptides. *Cell. Mol. Life Sci.* **73**, 271-290
5. Brogiolo, W., Stocker, H., Ikeya, T., Rintelen, F., Fernandez, R., and Hafen, E. (2001) An evolutionarily conserved function of the *Drosophila* insulin receptor and insulin-like peptides in growth control. *Curr. biol.* **11**, 213-221
6. Kondo, H., Ino, M., Suzuki, A., Ishizaki, H., and Iwami, M. (1996) Multiple gene copies for bombyxin, an insulin-related peptide of the silkmoth *Bombyx mori*: structural signs for gene rearrangement and duplication responsible for generation of multiple molecular forms of bombyxin. *J. Mol. Biol*. **259**, 926-937
7. Sonksen, P., and Sonksen, J. (2000) Insulin: understanding its action in health and disease. *Br. J. Anaesth.* **85**, 69-79
8. Lin, X., and Smagghe, G. (2018) Roles of the insulin signaling pathway in insect development and organ growth. *Peptides*
9. Rintelen, F., Stocker, H., Thomas, G., and Hafen, E. (2001) PDK1 regulates growth through Akt and S6K in *Drosophila*. *Proc. Natl. Acad. Sci. U. S. A.* **98**, 15020-15025
10. Anderson, K. E., Coadwell, J., Stephens, L. R., and Hawkins, P. T. (1998) Translocation of PDK-1 to the plasma membrane is important in allowing PDK-1 to activate protein kinase B. *Curr. biol.* **8**, 684-691
11. Saltiel, A. R., and Kahn, C. R. (2001) Insulin signalling and the regulation of glucose and lipid metabolism. *Nature* **414**, 799-806
12. Matsuzaki, Y., Tamai, K., Kon, A., Sawamura, D., Uitto, J., and Hashimoto, I. (2003) Keratinocyte responsive element 3: analysis of a keratinocyte-specific regulatory sequence in the 230-kDa bullous pemphigoid antigen gene promoter. *J. Invest. Dermatol.* **120**, 308-312
13. Battiprolu, P. K., Gillette, T. G., Wang, Z. V., Lavandero, S., and Hill, J. A. (2010) Diabetic cardiomyopathy: mechanisms and therapeutic targets. *Drug. Discov. Today. Dis. Mech.* **7**, e135-e143
14. Cho, K. S., Lee, J. H., Kim, S., Kim, D., Koh, H., Lee, J., Kim, C., Kim, J., and Chung, J. (2001) *Drosophila* phosphoinositide-dependent kinase-1 regulates apoptosis and growth via the phosphoinositide 3-kinase-dependent signaling pathway. *Proc. Natl. Acad. Sci. U. S. A.* **98**, 6144-6149
15. Yun, H. M., Noh, S., and Hyun, S. (2017) Minocycline treatment suppresses juvenile development and growth by attenuating insulin/TOR signaling in *Drosophila* animal model. *Sci Rep*. **7**, 44724
16. Riddiford, L. M., Hiruma, K., Zhou, X., and Nelson, C. A. (2003) Insights into the molecular

basis of the hormonal control of molting and metamorphosis from *Manduca sexta* and *Drosophila melanogaster*. *Insect. Biochem. Mol. Biol.* **33**, 1327-1338

17. Thomas, H. E., Stunnenberg, H. G., and Stewart, A. F. (1993) Heterodimerization of the *Drosophila* ecdysone receptor with retinoid X receptor and ultraspiracle. *Nature* **362**, 471-475
18. Yao, T. P., Segraves, W. A., Oro, A. E., McKeown, M., and Evans, R. M. (1992) *Drosophila* ultraspiracle modulates ecdysone receptor function via heterodimer formation. *Cell* **71**, 63-72
19. Lan, Q., Hiruma, K., Hu, X., Jindra, M., and Riddiford, L. M. (1999) Activation of a delayed-early gene encoding MHR3 by the ecdysone receptor heterodimer EcR-B1-USP-1 but not by EcR-B1-USP-2. *Mol. Cell. Biol.* **19**, 4897-4906
20. Zhou, X., and Riddiford, L. M. (2002) Broad specifies pupal development and mediates the 'status quo' action of juvenile hormone on the pupal-adult transformation in *Drosophila* and *Manduca*. *Development* **129**, 2259-2269
21. Hakim, R. S., Baldwin, K., and Smagghe, G. (2010) Regulation of midgut growth, development, and metamorphosis. *Annu. Rev. Entomol.* **55**, 593-608
22. Baldwin, K. M., and Hakim, R. S. (1991) Growth and differentiation of the larval midgut epithelium during molting in the moth, *Manduca sexta*. *Tissue. Cell.* **23**, 411-422
23. Wang, J. L., Jiang, X. J., Wang, Q., Hou, L. J., Xu, D. W., Wang, J. X., and Zhao, X. F. (2007) Identification and expression profile of a putative basement membrane protein gene in the midgut of *Helicoverpa armigera*. *BMC Dev. Biol.* **7**, 76
24. Tettamanti, G., Grimaldi, A., Pennacchio, F., and de Eguileor, M. (2007) Lepidopteran larval midgut during prepupal instar: digestion or self-digestion? *Autophagy* **3**, 630-631
25. Mirth, C. K., and Riddiford, L. M. (2007) Size assessment and growth control: how adult size is determined in insects. *BioEssays* **29**, 344-355
26. McBrayer, Z., Ono, H., Shimell, M., Parvy, J. P., Beckstead, R. B., Warren, J. T., Thummel, C. S., Dauphin-Villemant, C., Gilbert, L. I., and O'Connor, M. B. (2007) Prothoracicotropic hormone regulates developmental timing and body size in *Drosophila*. *Dev. Cell.* **13**, 857-871
27. Koyama, T., Rodrigues, M. A., Athanasiadis, A., Shingleton, A. W., and Mirth, C. K. (2014) Nutritional control of body size through FoxO-Ultraspiracle mediated ecdysone biosynthesis. *Elife* **3**, 03091
28. Cai, M. J., Zhao, W. L., Jing, Y. P., Song, Q., Zhang, X. Q., Wang, J. X., and Zhao, X. F. (2016) 20-Hydroxyecdysone activates Forkhead box O to promote proteolysis during *Helicoverpa armigera* molting. *Development* **143**, 1005-1015
29. Shao, H. L., Zheng, W. W., Liu, P. C., Wang, Q., Wang, J. X., and Zhao, X. F. (2008) Establishment of a new cell line from lepidopteran epidermis and hormonal regulation on the genes. *PloS one* **3**, e3127
30. Liu, C. Y., Liu, W., Zhao, W. L., Wang, J. X., and Zhao, X. F. (2013) Upregulation of the expression of prodeath serine/threonine protein kinase for programmed cell death by steroid hormone 20-hydroxyecdysone. *Apoptosis* **18**, 171-187
31. Kroemer, G., Galluzzi, L., Vandenabeele, P., Abrams, J., Alnemri, E. S., Baehrecke, E. H., Blagosklonny, M. V., El-Deiry, W. S., Golstein, P., Green, D. R., Hengartner, M., Knight, R. A., Kumar, S., Lipton, S. A., Malorni, W., Nunez, G., Peter, M. E., Tschopp, J., Yuan, J., Piacentini, M., Zhivotovsky, B., and Melino, G. (2009) Classification of cell death: recommendations of the Nomenclature Committee on Cell Death 2009. *Cell. Death. Differ* **16**, 3-11
32. Vilaplana, L., Pascual, N., Perera, N., and Belles, X. (2007) Molecular characterization of an

inhibitor of apoptosis in the Egyptian armyworm, *Spodoptera littoralis*, and midgut cell death during metamorphosis. *Insect. Biochem. Mol. Biol.* **37**, 1241-1248

33. Shpilka, T., Weidberg, H., Pietrokovski, S., and Elazar, Z. (2011) Atg8: an autophagy-related ubiquitin-like protein family. *Genome Biol*. **12**, 226
34. Li, Y. B., Li, X. R., Yang, T., Wang, J. X., and Zhao, X. F. (2016) The steroid hormone 20-hydroxyecdysone promotes switching from autophagy to apoptosis by increasing intracellular calcium levels. *Insect Biochem. Mol. Biol.* **79**, 73-86
35. Zhou, Z., Li, Y., Yuan, C., Zhang, Y., and Qu, L. (2015) Oral Administration of TAT-PTD-Diapause Hormone Fusion Protein Interferes With *Helicoverpa armigera* (Lepidoptera: Noctuidae) Development. *J. Insect Sci*. **15**, 123
36. Rabinowitz, J. D., and White, E. (2010) Autophagy and metabolism. *Science* **330**, 1344-1348
37. Tavallai, S., Hamed, H. A., Grant, S., Poklepovic, A., and Dent, P. (2014) Pazopanib and HDAC inhibitors interact to kill sarcoma cells. *Cancer Biol. Ther.* **15**, 578-585
38. Xiao, Y., Ma, C., Yi, J., Wu, S., Luo, G., Xu, X., Lin, P. H., Sun, J., and Zhou, J. (2015) Suppressed autophagy flux in skeletal muscle of an amyotrophic lateral sclerosis mouse model during disease progression. *Physiol. Rep.* **3**, e12271.
39. Kasprzak, A., Kwasniewski, W., Adamek, A., and Gozdzicka-Jozefiak, A. (2017) Insulin-like growth factor (IGF) axis in cancerogenesis. *Mutat. Res. Rev. Mutat. Res.* **772**, 78-104
40. Matsui, H., Kakei, M., Iwami, M., and Sakurai, S. (2012) Hormonal regulation of the death commitment in programmed cell death of the silkworm anterior silk glands. *J. Insect Physiol.* **58**, 1575-1581
41. Colombani, J., Bianchini, L., Layalle, S., Pondeville, E., Dauphin-Villemant, C., Antoniewski, C., Carre, C., Noselli, S., and Leopold, P. (2005) Antagonistic actions of ecdysone and insulins determine final size in *Drosophila*. *Science* **310**, 667-670
42. Kumar, D., Subrahmanyam, B., Sharan, S. K., Mishra, P. K., Singh, B. M. K., and Suryanarayana, N. (2008) Endogenous 20-hydroxyecdysone levels in the haemolymph of non-diapause-destined and diapause-destined generations of tasar silkworm, *Antheraea mylitta* (Lepidoptera: Saturniidae) and associated developmental changes. *Eur. J. Entomol.* **105**, 591-598
43. Xie, K., Tian, L., Guo, X., Li, K., Li, J., Deng, X., Li, Q., Xia, Q., Zhong, Y., Huang, Z., Liu, J., Li, S., Yang, W., and Cao, Y. (2016) BmATG5 and BmATG6 mediate apoptosis following autophagy induced by 20-hydroxyecdysone or starvation. *Autophagy* **12**, 381-396
44. Tettamanti, G., Grimaldi, A., Casartelli, M., Ambrosetti, E., Ponti, B., Congiu, T., Ferrarese, R., Rivas-Pena, M. L., Pennacchio, F., and Eguileor, M. (2007) Programmed cell death and stem cell differentiation are responsible for midgut replacement in *Heliothis virescens* during prepupal instar. *Cell Tissue Res.* **330**, 345-359
45. Tian, L., Ma, L., Guo, E. E., Deng, X. J., Ma, S. Y., Xia, Q. Y., Cao, Y., and Li, S. (2013) 20-hydroxyecdysone upregulates Atg genes to induce autophagy in the *Bombyx* fat body. *Autophagy* **9**, 1172-1187
46. Puig, O., Marr, M. T., Ruhf, M. L., and Tjian, R. (2003) Control of cell number by *Drosophila* FOXO: downstream and feedback regulation of the insulin receptor pathway. *Genes Dev.* **17**, 2006-2020
47. Hossain, M. S., Liu, Y., Zhou, S., Li, K., Tian, L., and Li, S. (2013) 20-Hydroxyecdysone-induced transcriptional activity of FoxO upregulates brummer and acid

lipase-1 and promotes lipolysis in *Bombyx* fat body. *Insect Biochem. Mol. Biol.* **43**, 829-838

48. Giannakou, M. E., Goss, M., Junger, M. A., Hafen, E., Leevers, S. J., and Partridge, L. (2004) Long-lived *Drosophila* with overexpressed dFOXO in adult fat body. *Science* **305**, 361
49. Hwangbo, D. S., Gershman, B., Tu, M. P., Palmer, M., and Tatar, M. (2004) *Drosophila* dFOXO controls lifespan and regulates insulin signalling in brain and fat body. *Nature* **429**, 562-566
50. Lapierre, L. R., Kumsta, C., Sandri, M., Ballabio, A., and Hansen, M. (2015) Transcriptional and epigenetic regulation of autophagy in aging. *Autophagy* **11**, 867-880
51. Urbich, C., Knau, A., Fichtlscherer, S., Walter, D. H., Bruhl, T., Potente, M., Hofmann, W. K., de Vos, S., Zeiher, A. M., and Dimmeler, S. (2005) FOXO-dependent expression of the proapoptotic protein Bim: pivotal role for apoptosis signaling in endothelial progenitor cells. *FASEB J.* **19**, 974-976
52. Zhang, X., Tang, N., Hadden, T. J., and Rishi, A. K. (2011) Akt, FoxO and regulation of apoptosis. *Biochim. Biophys. Acta* **1813**, 1978-1986
53. Wang, D., Pei, X. Y., Zhao, W. L., and Zhao, X. F. (2016) Steroid hormone 20-hydroxyecdysone promotes higher calcium mobilization to induce apoptosis. *Cell Calcium* **60**, 1-12
54. Keshan, B., Thounaojam, B., and Kh, S. D. (2017) Insulin and 20-hydroxyecdysone action in *Bombyx mori*: Glycogen content and expression pattern of insulin and ecdysone receptors in fat body. *Gen. Comp. Endocrinol.* **241**, 108-117
55. Liu, C. Y., Zhao, W. L., Wang, J. X., and Zhao, X. F. (2015) Cyclin-dependent kinase regulatory subunit 1 promotes cell proliferation by insulin regulation. *Cell Cycle*, 1-13
56. Orme, M. H., and Leevers, S. J. (2005) Files on steroids: The interplay between ecdysone and insulin signaling. *Cell Metab.* **2**, 277-278
57. Zhao, X. F., Wang, J. X., and Wang, Y. C. (1998) Purification and characterization of a cysteine proteinase from eggs of the cotton boll worm, *Helicoverpa armigera*. *Insect Bioch. Mol. Biol.* **28**, 259-264
58. Chen, C. H., Pan, J., Di, Y. Q., Liu, W., Hou, L., Wang, J. X., and Zhao, X. F. (2017) Protein kinase C delta phosphorylates ecdysone receptor B1 to promote gene expression and apoptosis under 20-hydroxyecdysone regulation. *Proc. Natl. Acad. Sci. U. S. A.* **114**, E7121-E7130
59. Liu, W., Cai, M. J., Zheng, C. C., Wang, J. X., and Zhao, X. F. (2014) Phospholipase cgamma1 connects the cell membrane pathway to the nuclear receptor pathway in insect steroid hormone signaling. *J. Biol. Chem.* **289**, 13026-13041
60. Xu, J., Wang, X. F., Chen, P., Liu, F. T., Zheng, S. C., Ye, H., and Mo, M. H. (2016) RNA interference in moths: mechanisms, applications, and progress. *Genes (Basel)* **7**, E88
61. Fire, A., Xu, S., Montgomery, M. K., Kostas, S. A., Driver, S. E., and Mello, C. C. (1998) Potent and specific genetic interference by double-stranded RNA in *Caenorhabditis elegans*. *Nature* **391**, 806-811
62. Zamore, P. D., Tuschl, T., Sharp, P. A., and Bartel, D. P. (2000) RNAi: double-stranded RNA directs the ATP-dependent cleavage of mRNA at 21 to 23 nucleotide intervals. *Cell* **101**, 25-33
63. Zhao, W. L., Liu, C. Y., Liu, W., Wang, D., Wang, J. X., and Zhao, X. F. (2014) Methoprene-tolerant 1 regulates gene transcription to maintain insect larval status. *J. Mol. Endocrinol*. **53**, 93-104
64. Sui, Y. P., Wang, J. X., and Zhao, X. F. (2009) The impacts of classical insect hormones on the

expression profiles of a new digestive trypsin-like protease (TLP) from the cotton bollworm, *Helicoverpa armigera*. *Insect Mol. Biol.* **18**, 443-452

65. Baehrecke, E. H. (2005) Autophagy: dual roles in life and death? *Nat. Rev. Mol. Cell Biol.* **6**, 505-510

66. Li, Y. B., Pei, X. Y., Wang, D., Chen, C. H., Cai, M. J., Wang, J. X., and Zhao, X. F. (2017) The steroid hormone 20-hydroxyecdysone upregulates calcium release-activated calcium channel modulator 1 expression to induce apoptosis in the midgut of *Helicoverpa armigera*. *Cell Calcium* **68**, 24-33

Table 1. Oligonucleotide sequences of the PCR primers

Primer name	Sequence (5′-3′)
qRT-PCR	
PDK1-RTF	ACAGCACCGTGTTTCTTGC
PDK1-RTR	GCGTCTTTCTCGCGTTTA
AKT-RTF	CATCATACAGAAGGACGAGGTGG
AKT-RTR	GCGACAGGTGGAAGAACAGC
FoxO-RTF	TCATTACCCAAGCCAGCAC
FoxO-RTR	TCCATCCAGCCGAAGAGT
β-actin RTF	CCTGGTATTGCTGACCGTATGC
β-actin RTR	CTGTTGGAAGGTGGAGAGGGAA
RNAi	
PDK1RNAiF	GCGTAATACGACTCACTATAGGGGCGGCTGAGTTGTTGATGG
PDK1RNAiR	GCGTAATACGACTCACTATAGGGCGGGCTAATAGTCGGTGGC
Overexpression	
AKT-oexF	TACTCATACTCAAGATCTCGATGGCGGAGGCGGCGCCCG
AKT-oexR	TACTCATACTCAGTCGACCTGGCGCTTGTCAGCCAGC
FoxO-oexF	TACTCATACTCAGAGCTCATGTCTATACGGGGCAGC
FoxO-oexR	TACTCATACTCAAGATCTGGTGGACCCAGGAGGGGGC

Figure legends

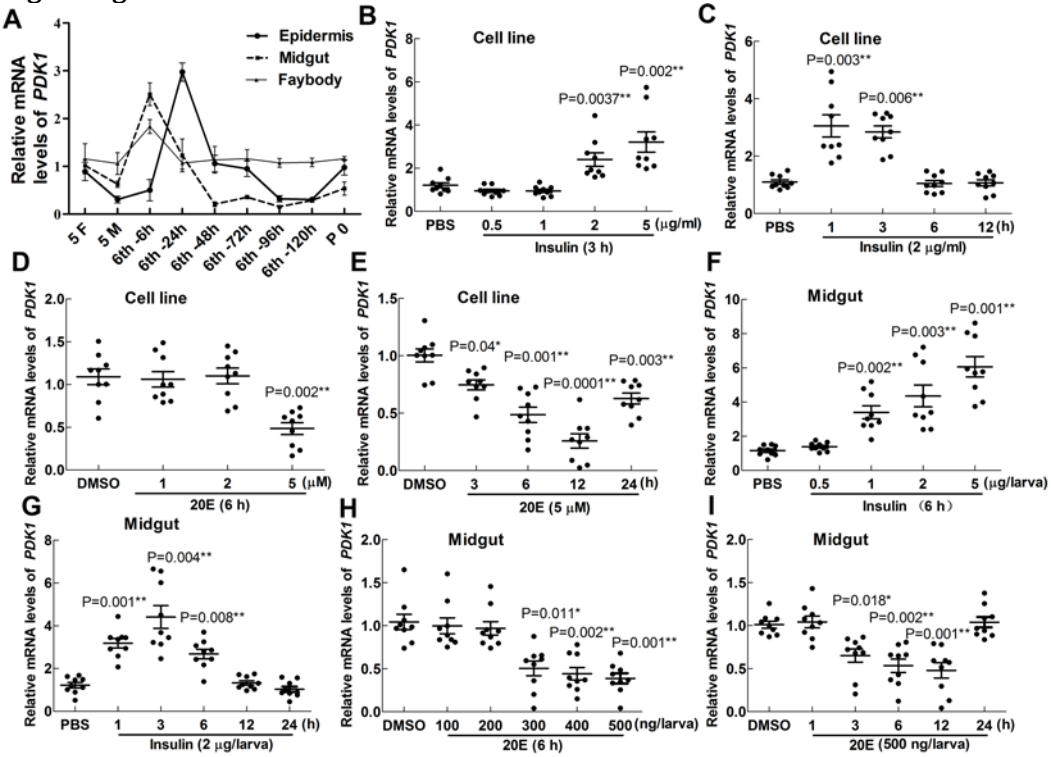

Figure 1 qRT-PCR showing the expression profile and hormonal regulation of *PDK1*. (A) The expression profile of *PDK1* in *H. armigera* larval tissues. **5 F:** 5th-instar feeding larvae; 5 **M:** 5th-instar molting larvae; **6th-6h to 6th-120h:** time stages of 6th instar larvae; **P0:** pupation 0 h. **(B)** The expression of *PDK1* in HaEpi cells by insulin (0.5–5 μg/ml) induction for 3 h. PBS was used as the solvent control. **(C)** The expression of *PDK1* in HaEpi cells by insulin (2 μg/ml) induction (1–12 h,). PBS was used as the solvent control. **(D)** The expression of *PDK1* in HaEpi cells by 20E induction (1–5 μM for 6 h). **(E)** The expression of *PDK1* in HaEpi cells by 20E (5 μM) induction (3–24 h). DMSO was used as the solvent control. **(F)**, **(G)**, **(H)** and **(I)** Hormonal regulation of the expression of *PDK1* in the larval midgut. All of the experiments were performed in triplicate, and statistical analysis was conducted using Student's *t*-test. The bars indicate mean ± SD. The asterisks indicate the significant differences when compared with PBS or DMSO.

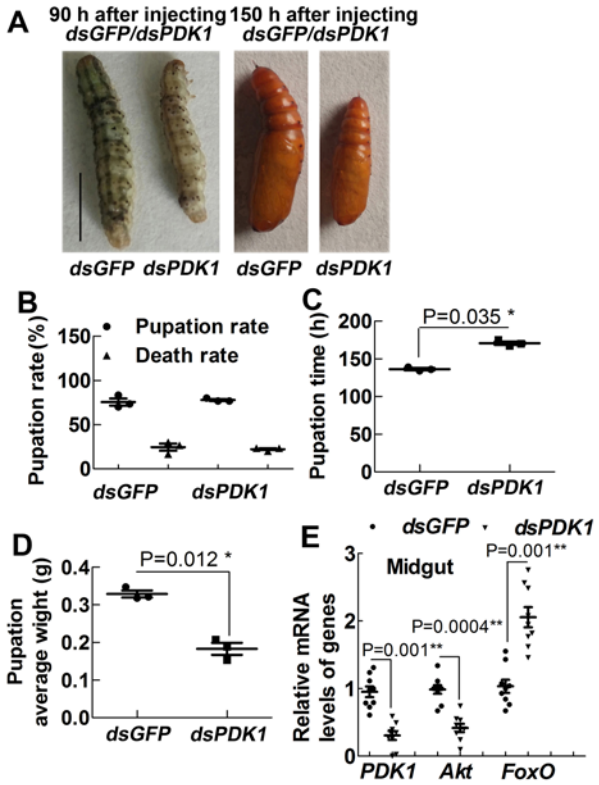

Figure 2 Knockdown of *PDK1* delayed pupation time and decreased body weight. (A) Phenotypes after *dsPDK1* or *dsGFP* injection (2 μg/6th instar 6 h larva). The bar represents 1 cm. **(B)** Analysis of the pupation rate and death rate by using Student's *t*-test; The bars indicate mean ± SD based 3 repeats, with 30 larvae in a repeat, respectively. **(C)** The time in which half of the larvae pupated after *dsGFP* or *dsPDK1* injection. **(D)** Statistical analysis of average body weight of a pupa at day one, by individually weighed, after *PDK1* knockdown by injection with *dsGFP* or *dsPDK1*. **(E)** The efficacy of *PDK1* knockdown and transcript levels of *AKT* and *FoxO* in the larval midgut at 90 h after first dsRNA injection. All the experiments were performed in triplicate, and statistical analysis was conducted using Student's *t*-test. The bars indicate mean ± SD.

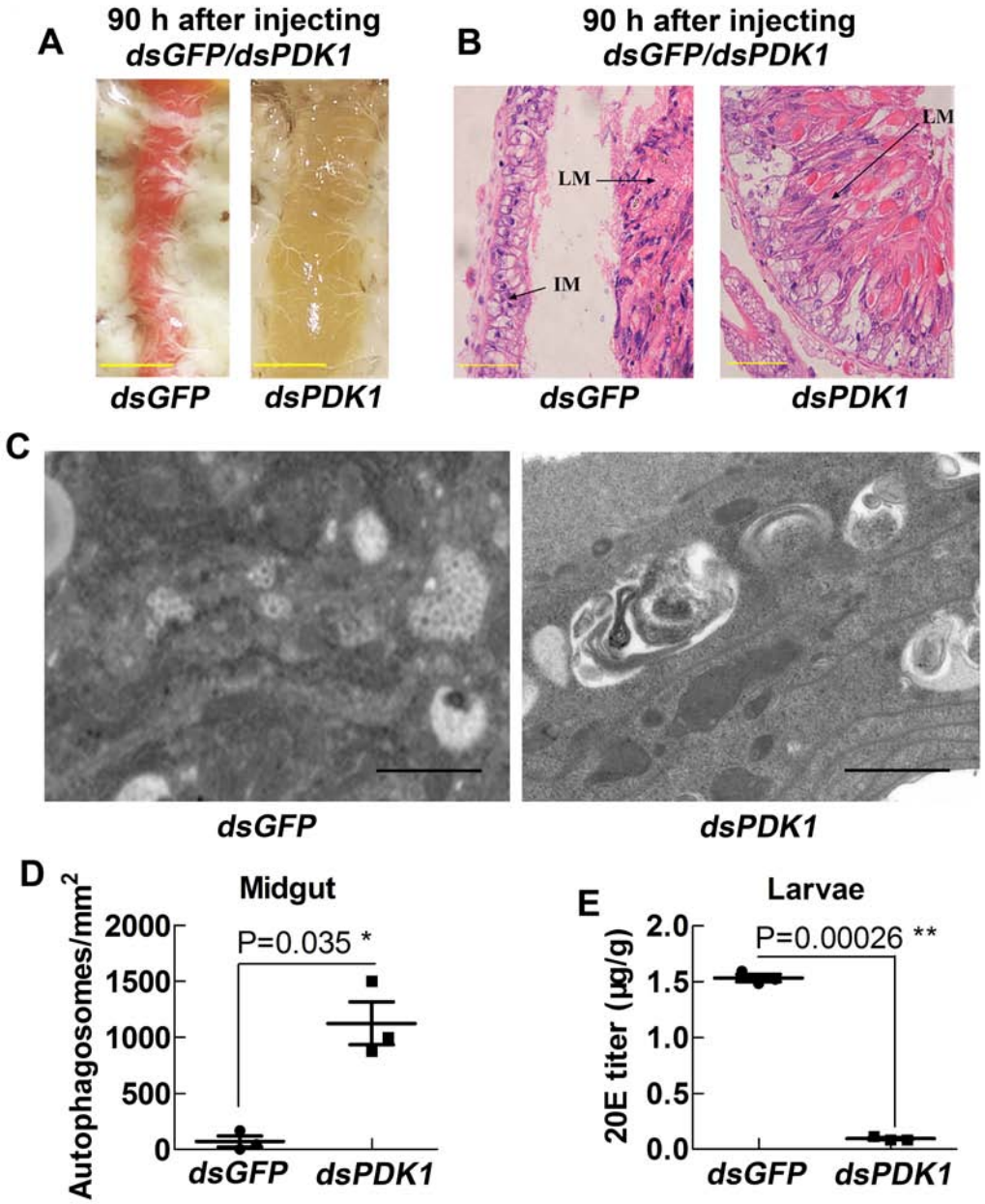

Figure 3 Knockdown of *PDK1* in larvae repressed midgut remodeling and decreased 20E levels. (A) Midgut morphology after injection with *dsGFP* or *dsPDK1* for 90 h. The bar represents 1 cm. **(B)** HE-stained midgut cross slides after knockdown of *PDK1*, observed at 90 h after dsRNA injection. **LM:** larval midgut; **IM:** imaginal midgut. The bars represent 10 μm. **(C)** TEM observation after injection with dsGFP or dsPDK1 for 90 h in the midgut. The bars represent 10 μm. **(D)** Statistical analysis of the autophagosomes in C by using Student's *t*-test based on three independent replicates. We counted the autophagosomes according to the scale. **(E)** 20E levels detected in larvae 90 h after injection with *dsGFP* or *dsPDK1*. All the experiments were performed in triplicate, and statistical analysis was conducted using Student's *t*-test based on three independent replicates.

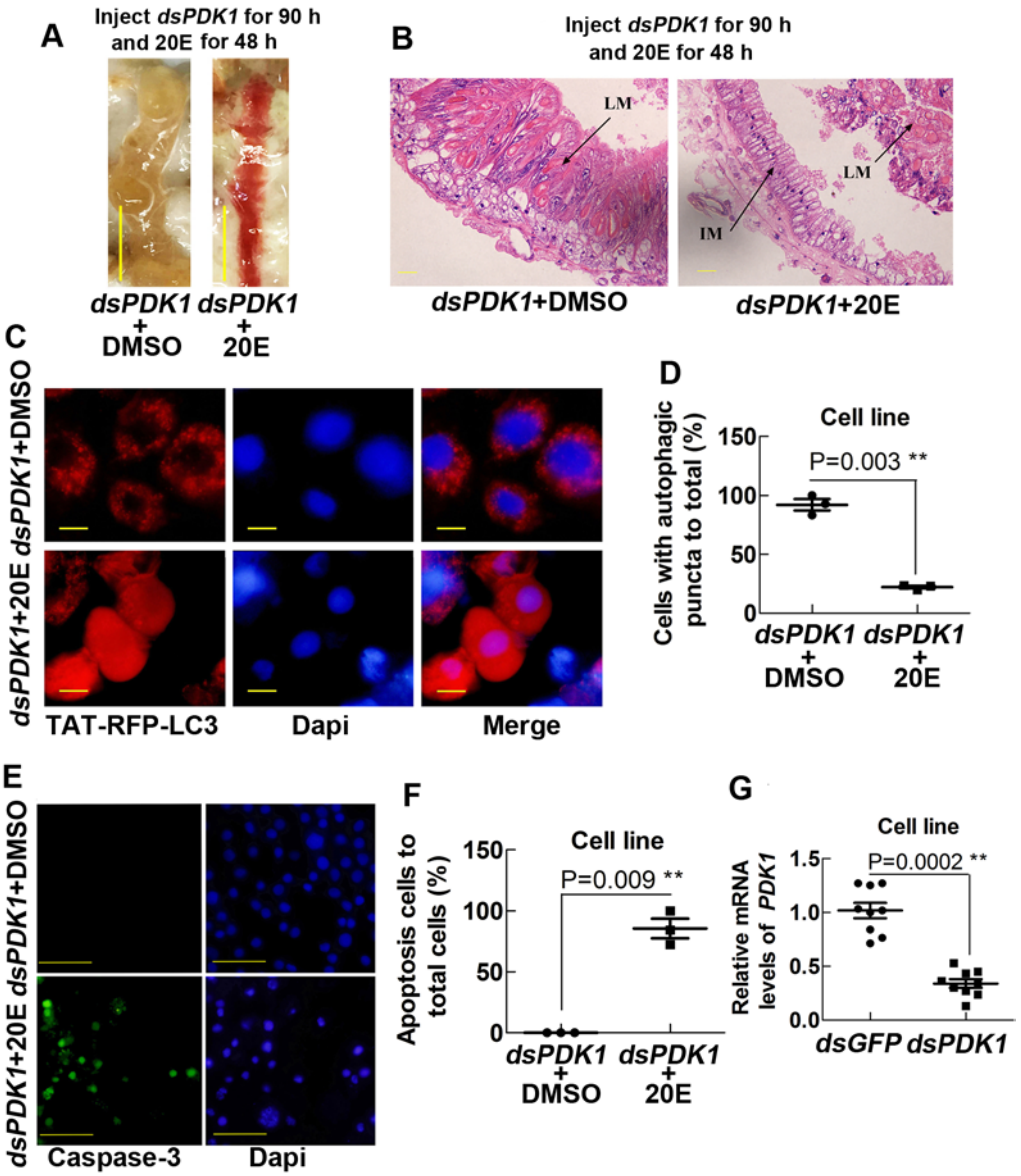

Figure 4 20E rescued the effect of *PDK1* knockdown. (A) The morphology of the midgut after injection with *dsPDK1* for 90 h and then injection with DMSO or 500 ng 20E for 48 h. DMSO was used as the solvent control. The bar represents 1 cm. **(B)** The histology of the midgut after the treatment mentioned in **A**. **LM:** larval midgut, **IM:** imaginal midgut. The bars represent 10 μm. **(C)** Examination of autophagy in HaEpi after *PDK1* knockdown by using TAT-RFP-LC3 to indicate the vesicles of autophagosomes. DMSO or 20E (5 μM) treatment for 72 h. Red: TAT RFP-LC3; Blue: nucleus stained with DAPI; Merge: overlapping red and blue. The yellow bars represent 20 μm. **(D)** Statistical analysis of (C) by using the data from 100 × 3 cells. The ratio between the cells in autophagy (red) to the total cells (blue) in the field view was obtained. **(E)** Examination of apoptosis in HaEpi cells after *PDK1* knockdown by using the NucView™ caspase-3 activity assay kit. DAPI stained the nucleus (blue fluorescence). The yellow bars represent 50 μm. **(F)** Statistical analysis of (E) by using the data from 100 × 3 cells. The ratio of the cells in apoptosis (green) to the total cells (blue) in the field view was obtained. **(G)** Efficiency of interference in the HaEpi cell line. All the experiments were performed in triplicate, and statistical analysis was conducted using Student's *t*-test. The bars indicate mean ± SD.

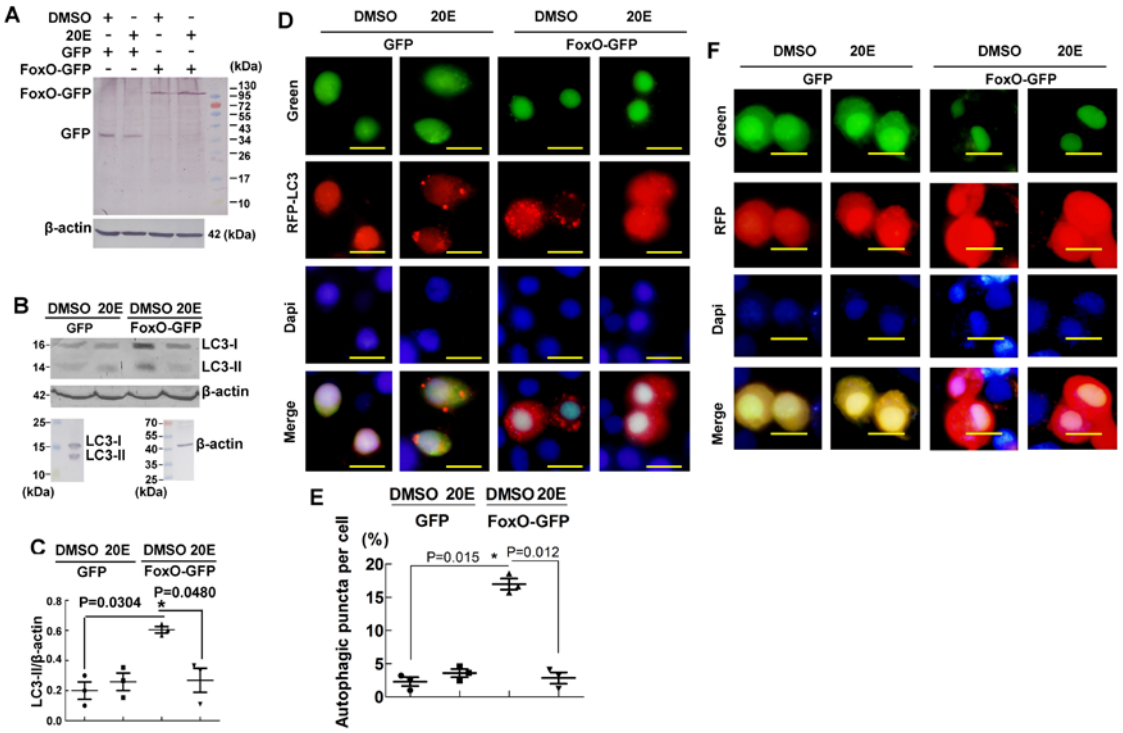

Figure 5 Overexpression of FoxO induced autophagy. (A) Western blot showing the overexpression of GFP-His and FoxO-GFP-His in HaEpi cells for 48 h and DMSO or 20E (5 μM) treatment for 72 h. The SDS gel concentration was 12.5%; β-actin was used as the internal reference. **(B)** Western blot assay of LC3-I and LC3-II levels in HaEpi; β-actin was used as the internal reference. The SDS gel concentration was 12.5%. **(C)** Statistical analysis of (B) using Student's *t*-test based on three independent replicates. **(D)** Micrograph of cells. Transfection with 2 μg pIEx-RFP-LC3-His plasmid for 48 h to indicate autophagy before the treatments. RFP-LC3: RFP-LC3-His. Green: GFP-His or FoxO-GFP-His. Blue: nucleus stained with DAPI; Red: RFP-LC3 or RFP; Merge: overlapping red, green, and blue. Bar: 20 μm. **(E)** Statistical analysis of (D) by using the data from 100 × 3 cells. The ratio of the number of autophagy puncta to the number of cells (red cells) was obtained. All the experiments were performed in triplicate, and statistical analysis was conducted using Student's *t*-test. Bars represent mean ± SD. **(F)** Micrograph of cells for the negative control for (D) by overexpression of the RFP-tag. Bar: 20 μm.

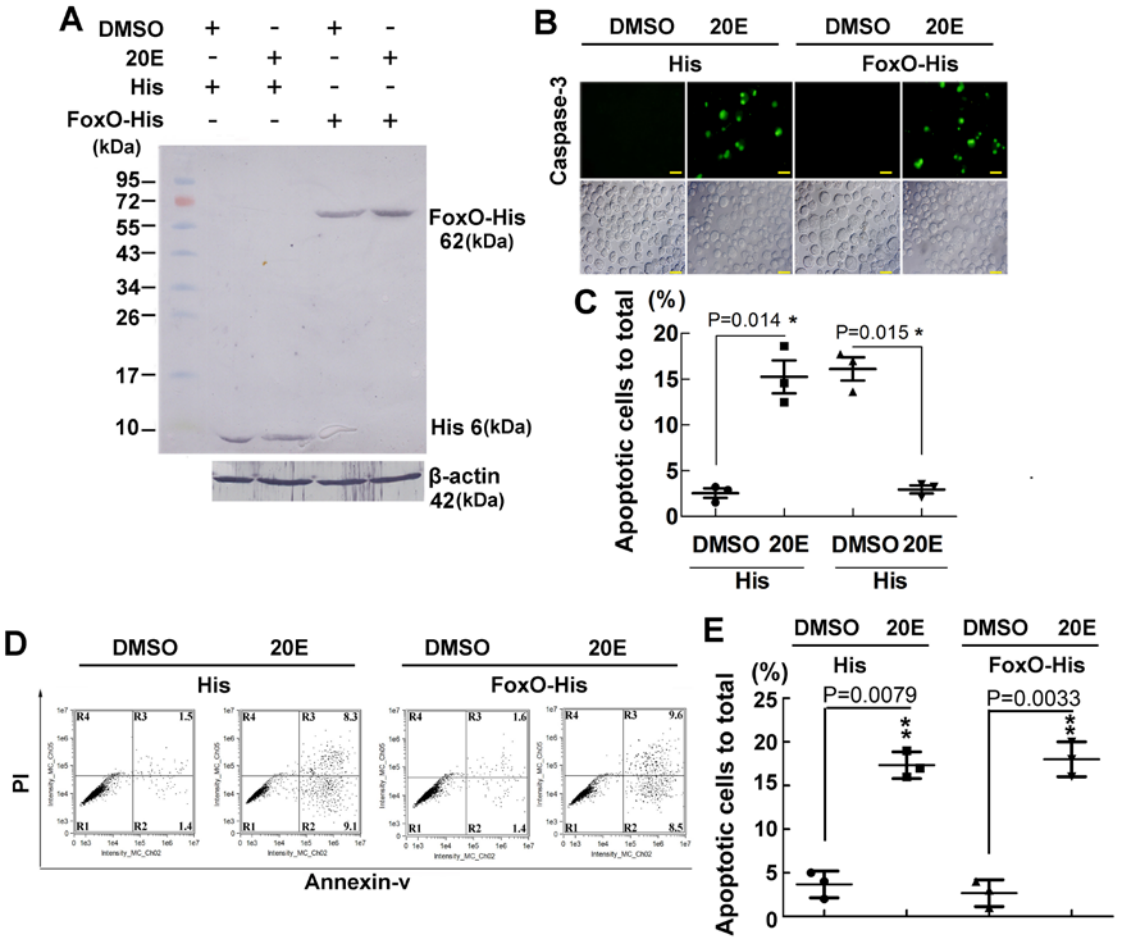

Figure 6 Overexpression of FoxO could not induce apoptosis without 20E induction. (A) Western blot showing the overexpression of His-tag and FoxO-His in HaEpi. SDS gel concentration was 12.5%. **(B)** Caspase-3 activity (green fluorescence) was detected using the NucView^{TM} caspase-3 activity assay kit after stimulation with DMSO or 20E (5 μM) for 72 h. Bar: 20 μm. Other treatments were the same as in (A). There is no difference in FoxO-overexpression in the presence/absence of 20E and that the effect of 20E is the same regardless of the overexpression of FoxO. **(C)** Statistical analysis of (B) by using the data from 100 cells. The ratio of the cells in apoptosis (green) to the total cells (white) in the field view was obtained by using Student's *t*-test on the basis of three independent replicates. Bars represent mean ± SD. **(D)** Flow cytometry analysis of annexin-V and propidium iodide (PI) staining after the same treatments as in (A). Annexin V-FITC stained the earlier apoptotic cells by binding to the membrane phosphatidylserine, and PI indicated the later apoptotic cells and dead cells by entering the cells. R1, normal cells; R2, early apoptotic cells; R3, middle and late apoptotic cells; R4, dead cells. The numbers in the figure mean the percentage of apoptotic cells. **(E)** Statistical analysis of (D). All the experiments were performed in triplicate, and statistical analysis was conducted using Student's *t*-test. Bars represent mean ± SD.

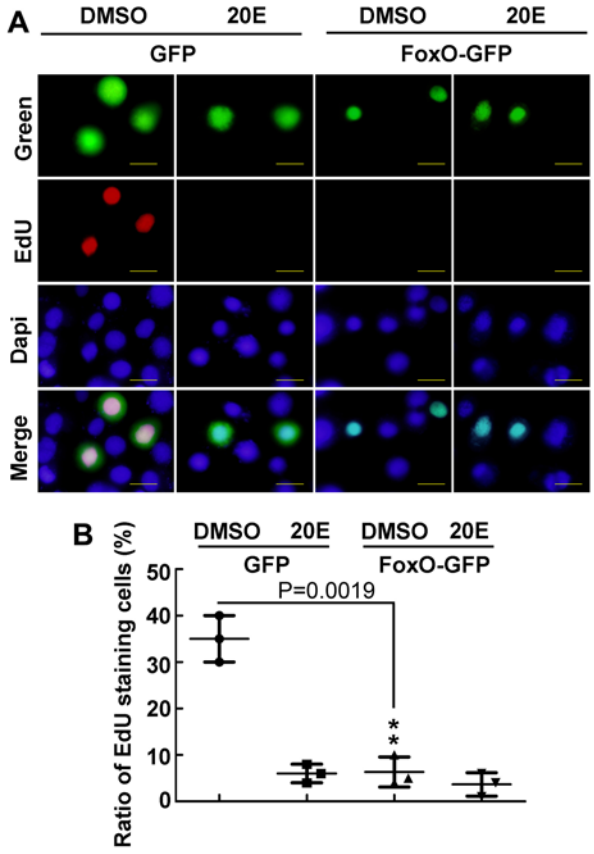

Figure 7 Overexpression of FoxO repressed cell proliferation. (A) Overexpression of GFP-His and FoxO-GFP-His in HaEpi cells and detection of cell proliferation by EdU. Green: GFP-His or FoxO-GFP-His. β-actin was used as the internal reference. Treatment of the cells with 20E (5 μM) for 72 h. The same volume of DMSO was used as the control. Blue: nucleus stained with DAPI; Red: EdU; Merge: overlapping red, green, and blue. Bar: 20 μm. **(B)** Statistical analysis of (A) by using the data from 100 × 3 cells. All the experiments were performed in triplicate, and statistical analysis was conducted using Student's *t*-test. Bars represent mean ± SD.

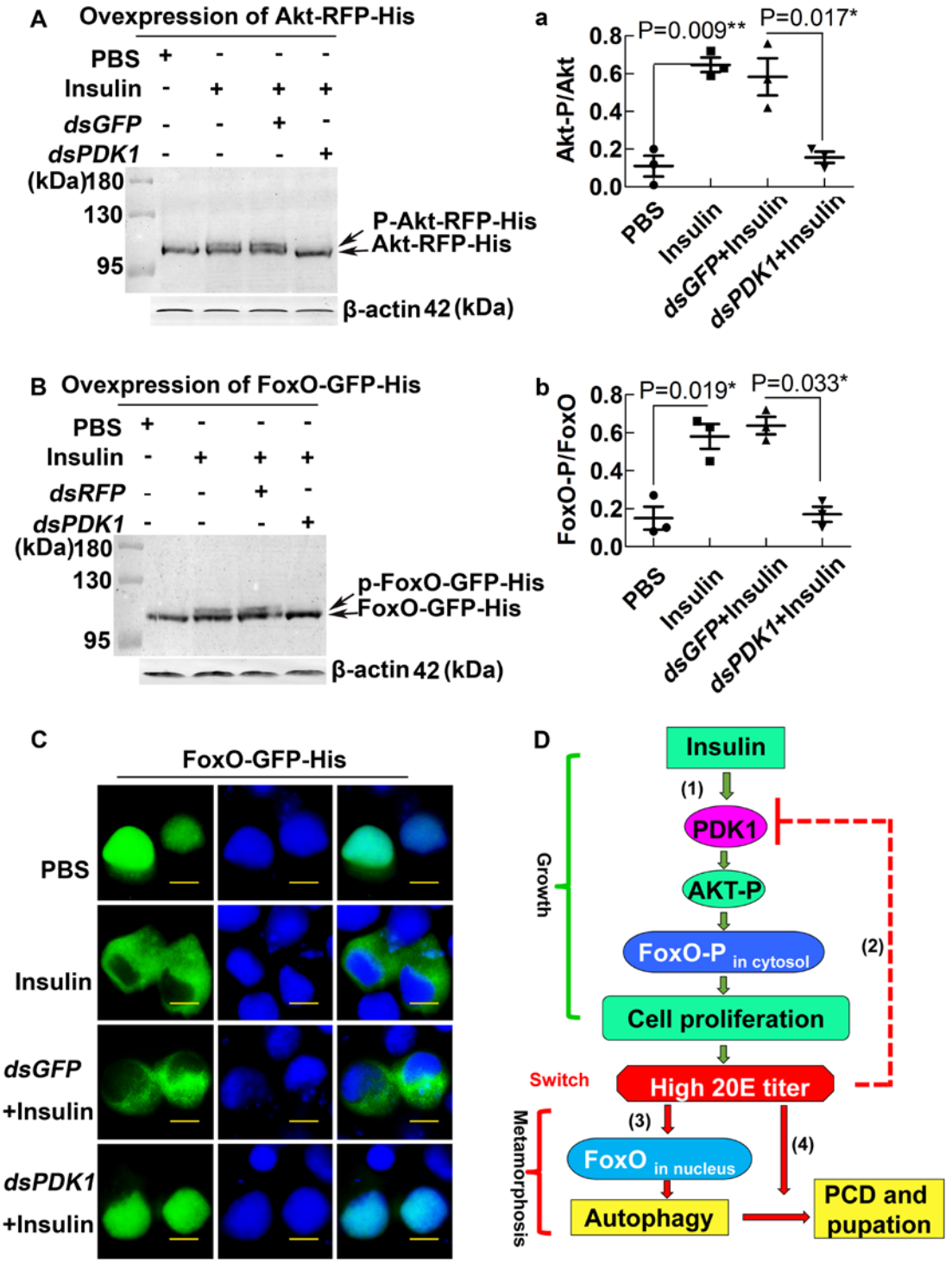

Figure 8 PDK is involved in insulin pathway. (A) and **(B)** Insulin, via PDK1, induces Akt and FoxO phosphorylation. The cells were transfected with Akt-RFP-His or FoxO-GFP-His for 48 h and then transfected with 2 μg of *dsGFP* or *dsPDK1*. Insulin (5 μg/mL) was added to the cells in DPBS for 1 h. 7.5% SDS-PAGE was performed, with β-actin as the control. P-Akt-RFP-His and P-FoxO-GFP-His are the phosphorylated forms of the proteins, respectively. **(a)** and (**b)** Statistical analysis of (A) and (B). Akt-P: P-Akt-RFP-His, FoxO-P: P-FoxO-GFP-His. All experiments were performed in triplicate, and statistical analysis was conducted using Student's *t*-test. The bars represent mean ± SD. **(C)** *PDK1* knockdown blocked insulin-induced FoxO cytoplasmic translocation. Green fluorescence indicates FoxO-GFP-His. Blue, nuclei (DAPI). Scale bars: 20 μm. **(D)** Explanation for the regulation of pupation by insulin and 20E via counteractive regulation of *PDK1* expression. **(1)** Insulin

upregulates PDK1 expression, which induces Akt phosphorylation. Akt induces FoxO phosphorylation and cytosol localization to allow cell proliferation and high titer of 20E production. **(2)** High 20E titer represses PDK1 mRNA levels by an unknown negative feedback mechanism, therefore represses Akt and FoxO phosphorylation, resulting in FoxO nuclear localization. **(3)** FoxO in nucleus induces autophagy and represses cell proliferation. **(4)** 20E promotes autophagy transformed to apoptosis in the midgut during metamorphosis by increasing cellular calcium (34,53,66). High 20E titer functions as a switch between growth and metamorphosis. AKT-P: phosphorylated PDK. FoxO-P: phosphorylated FoxO. PCD: programmed cell death.

Insulin and 20-hydroxyecdysone oppose each other in the regulation of phosphoinositide-dependent kinase-1 expression during insect pupation

Jing Pan, Yu-Qin Di, Yong-Bo Li, Cai-Hua Chen, Jin-Xing Wang and Xiao-Fan Zhao

J. Biol. Chem. published online October 10, 2018
